Recent Strengthening of the Relationship between the Western North Pacific Monsoon and Western North Pacific Tropical Cyclone Activity during the Boreal Summer

HAIKUN ZHAO

Key Laboratory of Meteorological Disaster, Ministry of Education, and Joint International Research Laboratory of Climate and Environment Change, and Collaborative Innovation Center on Forecast and Evaluation of Meteorological Disaster, and Pacific Typhoon Research Center, Nanjing University of Information Science and Technology, Nanjing, China

SHAOHUA CHEN

Key Laboratory of Meteorological Disaster of Ministry of Education, Nanjing University of Information Science and Technology, Nanjing, China

PHILIP J. KLOTZBACH

Department of Atmospheric Science, Colorado State University, Fort Collins, Colorado

(Manuscript received 8 January 2019, in final form 31 July 2019)

ABSTRACT

This study examines the association between the western North Pacific (WNP) summer monsoon (WNPSM) and WNP tropical cyclone (TC) frequency during June–August from 1979 to 2016. The interannual relationship between the WNPSM and the total number of WNP TCs has strengthened since 1998. There has also been a significant reduction in the number of TCs forming within the WNP monsoon trough (WNPMT)—hereafter called ITCs, for internal or inside TCs—since 1998. These two important features are found to be closely associated with the climate regime shift that occurred around 1998. During 1998–2016, the Pacific decadal oscillation (PDO) tended to be in a cold phase, with an increasing occurrence of central Pacific–type El Niño–Southern Oscillation (ENSO) events, whereas the 1979–97 period tended to be characterized by a warm phase of the PDO and east Pacific–type ENSO events. During 1998–2016, the tropical Pacific was characterized by enhanced easterlies, which led to a westward-retreated WNPMT that caused a significant decrease in ITCs over the WNP basin. However, there was little change in TCs outside of the WNPMT region (hereafter called OTCs) compared to that before 1998. A significant in-phase (out-of-phase) relationship between the WNPSM and the number of ITCs (OTCs) is observed before 1998, thus greatly weakening the WNPSM–TC relationship. The recent enhanced relationship between the WNPSM and TCs is mainly due to a strong in-phase relationship between the WNPSM and ITCs. The interannual change in ITCs is mainly controlled by WNPSM changes since 1998, while OTC changes are mainly modulated by changes in the tropical upper-tropospheric trough.

1. Introduction

While significant progress over the past several decades has been made in understanding the physical mechanisms of changes in tropical cyclone (TC) activity on various time scales (Emanuel 2018; Walsh et al. 2015; Knutson et al. 2010), the prediction of TC genesis remains challenging (Xiang et al. 2015; Jiang et al. 2018). On average, about 1/3 of global TCs occur over the western North Pacific (WNP) (Chan 2005). These TCs post a threat both to human life and property over China and other East Asian countries (Zhang et al. 2009). Enhanced understanding of multiscale climate variability of TC genesis over the WNP basin therefore has important implications for WNP TC prediction and is therefore of great scientific merit.

TC genesis largely depends on a conducive large-scale environment [e.g., warm sea surface temperatures (SSTs), low vertical wind shear, high low-level relative vorticity, and high midlevel relative humidity] (Gray 1968, 1975, 1984; McBride and Zehr 1981; Shapiro 1987; Goldenberg and Shapiro 1996). Several TC genesis

Corresponding author: Dr. Haikun Zhao, zhk2004y@gmail.com

DOI: 10.1175/JCLI-D-19-0016.1

potential indices (GPIs) based on combinations of these large-scale factors have been developed (Gray 1979; Emanuel and Nolan 2004; Murakami and Wang 2010; Tippett et al. 2011), and these GPIs have been used to study variations of both TC genesis frequency and spatial distribution on various time scales (Camargo et al. 2007a,b, 2009; Vecchi and Soden 2007; Nolan et al. 2007; Lyon and Camargo 2009; Yokoi et al. 2009; Yokoi and Takayabu 2009; Jiang et al. 2012; Hsu et al. 2014; Zhao and Raga 2014, 2015; Zhao et al. 2015a,b, 2018a,b, 2019). The WNP summer monsoon (WNPSM) is considered to be one of the most important large-scale systems for breeding boreal summer (June–August) WNP TC genesis. Previous studies have suggested that about 70% of the total number of WNP TCs are associated with the WNP monsoon trough (WNPMT) (Gray 1968; Frank 1987; McBride 1995; Ritchie and Holland 1999; Harr and Chan 2005; Chen et al. 2006; Wu et al. 2012; Molinari and Vollaro 2013; Zong and Wu 2015a,b; Choi et al. 2016; Wang and Wu 2018). The importance of the WNPMT on TC genesis has been largely explained by two reasons. The first reason is that the WNPMT is characterized by a near-equatorial confluence zone between low-level easterly trade winds and westerly winds (Briegel and Frank 1997; Chan and Evans 2002; Tomita et al. 2004; Wu et al. 2012; Zong and Wu 2015a,b) that can supply the dynamic and thermodynamic conditions favorable for TC genesis. The second reason is that the WNPMT can provide necessary synoptic-scale precursors for TC genesis through barotropic wave accumulation associated with increasing local low-level convergence and/or relative vorticity (Wallace 1971; Reed and Recker 1971; Gray 1998; Shapiro 1977; Zehnder 1991; Ritchie 1995; Zehr 1992; Sobel and Maloney 2000; Dickinson and Molinari 2002; Aiyyer and Molinari 2003; Frank and Roundy 2006; Zhou and Wang 2007; Chen and Huang 2009; Zhao et al. 2016).

On interannual time scales, the WNPSM exhibits significant variability that largely regulates TC genesis location and TC frequency (Wang and Fan 1999; Wang et al. 1999, 2001; Wu and Wang 2000; Chou et al. 2003; Wang and Zhou 2008; Wu et al. 2012; Molinari and Vollaro 2013; Choi et al. 2016). For example, Wu et al. (2012) investigated the impact of interannual variability of the WNPMT on WNP TCs and found a strong dependence of interannual variability of WNP TC activity on the WNPMT location. When the WNPMT extends eastward (retreats westward), more (fewer) TCs are observed over the southeastern quadrant of the WNP. A strong association between El Niño–Southern Oscillation (ENSO) and the WNPSM has also been documented (Wang et al. 2001). There is a significant interannual shift in TC location associated with ENSO through changes in both the intensity and the location of the WNPSM (Lander 1994; Wang and Chan 2002; Camargo and Sobel 2005; Zhao et al. 2011). There is a southeastward shift in TC formation location over the WNP basin during El Niño events in agreement with an apparent southeastward extension of the WNPMT during warm ENSO events.

Additionally, the WNPSM has a pronounced influence on total WNP TC frequency. Recently, Choi et al. (2016) documented a significant correlation of 0.60 between WNP monsoon intensity and WNP TC frequency during the boreal summer (June–August) from 1977 to 2013. They further conducted composite analyses of large-scale factors between strong and weak WNPSM cases to explain the strong linkage. To our knowledge, the majority of prior research has emphasized the importance of the WNPSM in controlling WNP TC genesis based upon composite analyses of the total number of TCs between strong and weak WNPSM years (Ritchie and Holland 1999; Wang and Zhou 2008; Wu et al. 2012; Choi et al. 2016). These studies have not specifically distinguished between WNP TCs forming within the WNPMT (hereafter ITCs, for internal or inside TCs) or WNP TCs forming outside of the WNPMT (hereafter OTCs, for outside TCs).

Since the late 1990s, WNP TC activity has experienced a marked reduction (Maue 2011; Liu and Chan 2013; Hsu et al. 2014; Wang and Liu 2016; Zhao and Wang 2016, 2019; Han et al. 2016; Wang and Wu 2016; Hong et al. 2016; He et al. 2017; Huangfu et al. 2017; Hu et al. 2018). These studies have suggested that the reduction of TC activity over the WNP basin during recent decades is due to changes of atmospheric and oceanic factors associated with the large-scale circulation of the WNP [e.g., a weakened WNPSM and a westward shifted tropical upper-tropospheric trough (TUTT)] in response to a shift in the mean state. Since the late 1990s, there has been an increasing occurrence of central Pacific (CP) ENSO events and a switch from the warm to the cool phase of the Pacific decadal oscillation (PDO) (Zhao and Wang 2016, 2019; Kao and Yu 2009; Xiang et al. 2013; Cai et al. 2015; Wang et al. 2019). Associated with this climate regime shift have been changes in interannual remote teleconnections that are also associated with WNP TC activity [e.g., ENSO (Zhao and Wang 2019); the PDO (Zhao and Wang 2016); the North Atlantic Oscillation (NAO; Zhou and Cui 2014); the Arctic Oscillation (AO) (Cao et al. 2016); and the SST gradient between the southwest Pacific and the western Pacific warm pool (Zhao et al. 2016)]. These studies have primarily focused on the total number of WNP TCs and have not accounted for ITCs and OTCs over the WNP basin individually.

Motivated by these studies, several questions naturally arise from the changes in these teleconnections associated with the climate regime shift:

1) What is the interannual relationship between ITCs and OTCs over the WNP basin? Is the relationship between the WNPSM and ITCs and the relationship between the WNPSM and OTCs robust and significant? How do changes in the interannual variability of ITCs or OTCs contribute to the relationship between the WNPSM and the total number of TCs over the WNP basin?
2) Is there a corresponding interdecadal change in the interannual relationship between the WNPSM and the total number of WNP TCs? Have there been interdecadal changes in the interannual variability of OTCs and ITCs? What are the physical mechanisms driving these observed changes?

The remainder of this study is organized as follows. The data and methodology used in this study are described in section 2. Section 3 investigates interdecadal changes in both the interannual relationship between the WNPSM and the total number of WNP TCs as well as long-term changes in the WNPSM and the total number of WNP TCs. Section 4 explores plausible physical mechanisms for these changes. Section 5 gives a summary and discussion.

2. Data and methodology

a. TC data: Atmospheric and oceanic datasets

Monthly atmospheric datasets are obtained from the National Centers for Environmental Prediction (NCEP)–Department of Energy (DOE) reanalysis with a horizontal resolution of 2.5° × 2.5° and 17 vertical levels (Kanamitsu et al. 2002). Monthly SST data are taken from NOAA's Extended Reconstructed Sea Surface Temperature (ERSST), version 4 (ERSST v4), with a horizontal resolution of 2.0° × 2.0° (Huang et al. 2015; Liu et al. 2015).

TC data are obtained from the Joint Typhoon Warning Center (JTWC) best track dataset (Chu et al. 2002), which includes 6-hourly-interval latitude, longitude, and maximum sustained wind speed. All TCs with an intensity greater than or equal to 20 kt (i.e., ~10.3 m s^{-1}; 1 kt ≈ 0.51 m s^{-1}) are considered in this study, and the first location where the TC reached 20 kt is referred to as the TC formation location. To confirm the robustness of this result using the JTWC best track dataset, two other best track datasets (e.g., Shanghai Typhoon Institute/China Meteorological Administration and Japan Meteorological Agency) were also used, and there was broad consistency among the three best track datasets. Additionally, a stricter TC criterion of greater than or equal to 34 kt (~17.5 m s^{-1})—that used for a named tropical storm—was examined, and similar results between WNPSM and WNP TC frequency were obtained to those using the less strict TC definition of 20 kt. Unless specifically stated otherwise, we show results using the JTWC best track dataset and the less strict TC definition.

b. Definition of WNPSM intensity and identification of TC formation within the WNPMT

The interannual variation of WNPSM intensity is measured by the dynamical WNP monsoon index (WNPMI) defined by Wang and Fan (1999). It is calculated by the difference of 850-hPa westerlies between a southern region (5°–15°N, 100°–130°E) and a northern region (20°–30°N, 110°–140°E). Although the upper-level circulation or vertical wind shear (Wang et al. 2000) and the 850-hPa relative vorticity (Wu et al. 2012; Molinari and Vollaro 2013; Li et al. 2017) have also been used to represent the interannual variability of WNPSM intensity, studies have suggested that the WNPMI is a better dynamical circulation index. This index has also been widely used to study the variability of the WNPSM intensity in previous studies (Wang and Fan 1999; Wang et al. 2001; Wang and Zhou 2008; Choi et al. 2016). The WPNMI has a better representation of the strength of the tropical westerlies and the intensity of low-level relative vorticity associated with the Rossby wave response to the convective heat source over the Philippine Sea. Additionally, the WNPMI has its strongest signal in terms of boundary layer moisture convergence in regions away from the equator (Wang et al. 2001). To further test the sensitivity to the different definitions of the WNPSM, we use the 850-hPa relative vorticity index following Molinari and Vollaro (2013) to represent the WNPSM intensity and obtained similar results. A comparison of results using these two indices will be discussed later in this study.

In this study, a TC formation within the WNPMT is identified through the three steps outlined in Zong and Wu (2015a,b). First, the WNPMT axis is determined by both the line of the 850-hPa zero zonal wind and positive relative vorticity. Second, the area with successive tropical westerly winds (easterly winds) on both sides of the WNPMT axis and 850-hPa positive relative vorticity is examined to determine the WNPMT. Last, the determination of the eastern boundary of the WNPMT is checked over the previously identified areas where there is negative zonal stretching deformation at 850 hPa (i.e., du/dx). If a TC forms inside this area, it is identified as a TC formation event within the WNPMT (i.e., an ITC).

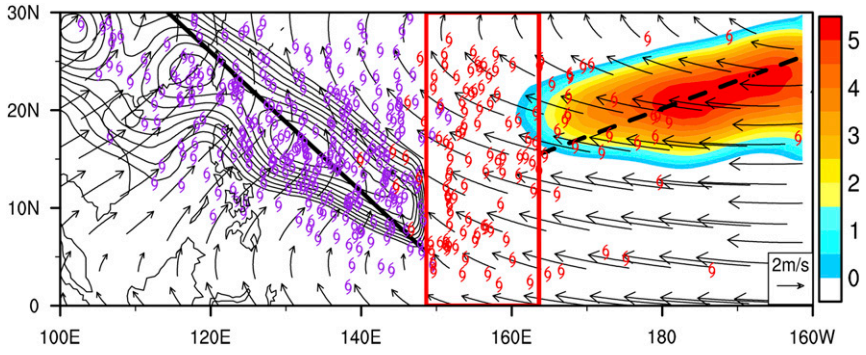

FIG. 1. Composite summer (JJA) 850-hPa wind (vectors) along with the averaged WNPMT (contours; $10^{-6}\,s^{-1}$) and TUTT (shading; $10^{-6}\,s^{-1}$) from 1979 to 2016. ITCs and OTCs are denoted by purple and red typhoon markers, respectively. The WNPMT and TUTT are identified by 850- and 200-hPa positive relative vorticity, respectively, relative to the composite JJA 850-hPa circulation. The solid (dashed) straight line is the annual average WNPMT (TUTT) axis, and the red box (0°–30°N, 148.5°–163.5°E) is the main development region for OTCs over the WNP basin.

If a TC forms outside of the WNPMT, it is referred to as a TC formation outside of the WNPMT (i.e., an OTC). Details on the identification of TC formation within the WNPMT can be found in Zong and Wu (2015a,b). Figure 1 shows the composite 850-hPa wind field during the boreal summer with respect to all of the annual WNPMTs along with the formation location of all ITCs and OTCs. The annual 200-hPa TUTT axis is determined as in the determination of the WNPMT axis discussed previously. Consistent with previous studies (Choi et al. 2016; Wu et al. 2015; Wang and Zhou 2008), ITC and OTC formations are closely linked to changes in both the WNPSM and the TUTT (Fig. 1). Using the classification outlined above, a majority of WNP TCs can be found within the WNPMT, in agreement with previous studies (Ritchie and Holland 1999; Wu et al. 2012; Molinari and Vollaro 2013; Zong and Wu 2015a). A total of 316 ITCs (~70% of the total JJA TC count) and 135 OTCs (~30% of the total JJA TC count) are identified over the WNP basin (Fig. 1). To examine the impact of changes in TUTT intensity, the averaged positive relative vorticity at 200 hPa over the main TUTT region from the western boundary of the annual TUTT axis to 140°W and 10°–35°N is used to define the TUTT intensity index (TUTTI). A similar definition for the TUTTI has been used in previous studies (Wu et al. 2015; Hu et al. 2018; Zhao et al. 2019).

c. *ENSO indices*

As has been suggested in previous studies that have investigated shifting ENSO conditions that began in the late 1990s (Kao and Yu 2009; Xiang et al. 2013; Cai et al. 2015; Zhao and Wang 2016, 2019), various ENSO indices including the Niño-3, Niño-3.4, and El Niño Modoki index (EMI) (Ashok et al. 2007) are used in this study to better understand the changes in interannual teleconnections associated with different ENSO flavors. Changes in the ENSO state have canonically been defined using the Niño-3.4 index, but this index does not well separate central Pacific (CP) and eastern Pacific (EP) ENSO events (Ashok et al. 2007). These two types of ENSO events show distinctly different teleconnected impacts on global climate and TC activity (e.g., Wang et al. 2014; Han et al. 2016) as well as other extreme weather events (Yu et al. 2012; Xiang et al. 2013; Cai et al. 2015; Zhao et al. 2016; Zhao and Wang 2016, 2018; Hu et al. 2018). The EMI has been adopted in many previous studies for representing CP ENSO events (Ashok et al. 2007; Kim et al. 2009; Chen and Tam 2010; Hong et al. 2011; Zhao et al. 2016; Zhao and Wang 2019). The EMI is calculated in Ashok et al. (2007) with the following expression:

$$\begin{aligned}\mathrm{EMI} = {} & \mathrm{SSTA}_{(10°\mathrm{S}–10°\mathrm{N},165°\mathrm{E}–140°\mathrm{W})} \\ & - 0.5\mathrm{SSTA}_{(10°\mathrm{S}–20°\mathrm{N},125°–145°\mathrm{E})} \\ & - 0.5\mathrm{SSTA}_{(15°\mathrm{S}–5°\mathrm{N},110°–70°\mathrm{W})}. \end{aligned} \quad (1)$$

d. *Statistical significance tests*

The statistical significance for the correlation and composite analysis is tested by a two-tailed Student's test. In this study, P values equal to or less than 0.05 are deemed statistically significant. The threshold correlation coefficients of significance are 0.46 for the two subperiods of 1979–97 (19 years) and 1998–2016 (19 years), and 0.32 for the whole period of 1979–2016 (38 years).

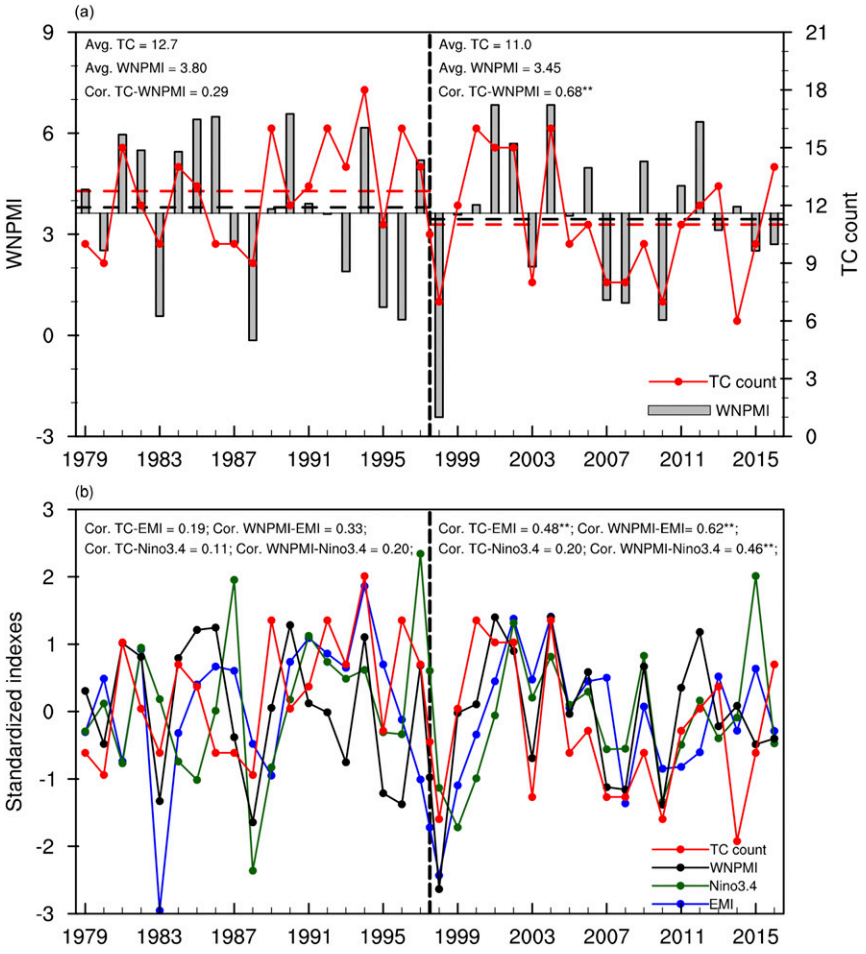

FIG. 2. (a) Time series of the boreal summer average WNPMI (gray bars) and total TC count (red solid line) during 1979–2016. The average WNPMI during 1979–97 and 1998–2016 is indicated by the black dashed line, and the average total TC count for these two subperiods is indicated by the red dashed line. The average for the two subperiods and the correlation coefficient between the total TC count and WNPMI during the two subperiods are also listed. (b) Time series of the standardized summer average WNPMI (black line), Niño-3.4 index (green line), EMI (blue line), and total TC count (red line). The correlation coefficients among the WNPMI, EMI, and Niño-3.4 index during the two subperiods are also listed. Double asterisks indicate statistical significance at a 95% confidence level.

3. On the relationship between the WNPSM and TC activity

a. In-phase interannual relationship between the WNPSM and TCs

Figure 2 shows the time series of the WNPMI, Niño-3.4 index, EMI, and total TC counts as well as the relationships between these time series. There is a significant positive correlation of 0.51 between the WNPMI and TC frequency over the entire WNP basin (Fig. 2a and Table 3), consistent with previous studies discussing the importance of the WNPSM as a breeding region for TCs (Holland 1995; Chen et al. 1998; Wang and Zhou 2008; Zhao et al. 2011; Molinari and Volaro 2013; Wu et al. 2012; Choi et al. 2016; Zong et al. 2015a,b). This in-phase WNPMT–TC relationship is further demonstrated when examining the composite differences of TC frequency over the WNP basin between eight strong WNPSM years (1981, 1985, 1986, 1990, 1994, 2001, 2004, 2012) and eight weak WNPSM years (1983, 1988, 1995, 1996, 1998, 2007, 2008, 2010) (Fig. 3). The years with a standardized WNPMI greater than 1 (less than –1) during the study period are referred to as strong (weak) WNPSM years. As shown in Fig. 3 and Table 1, the JJA average number of TCs is 13.9 during strong WNPSM years, whereas the JJA average TC number decreases to 9.5 during weak

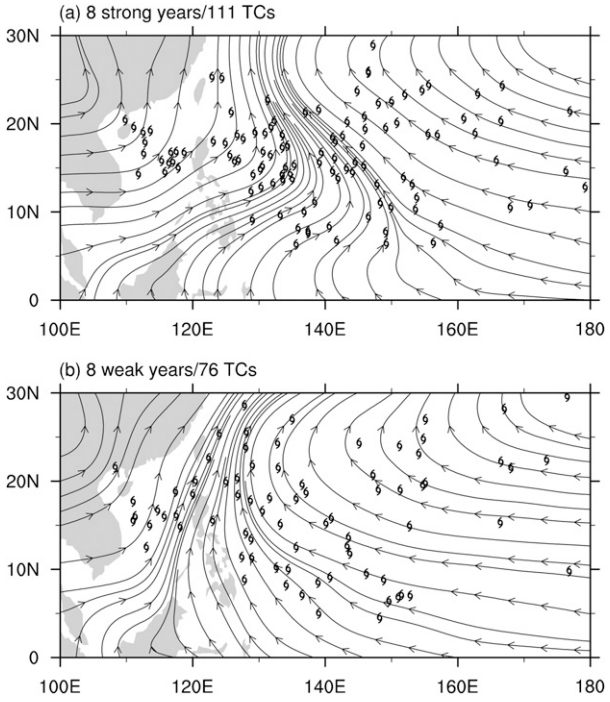

FIG. 3. Streamlines at 850 hPa averaged over the boreal summer (JJA) along with TC genesis locations for (a) strong and (b) weak WNP monsoon years during 1979–2016.

WNPSM years. This difference of 4.4 TCs between strong and weak WNPSM years is significant.

There has been a well-documented reduction of WNP TCs since the late 1990s (Fig. 2a, Table 2) (Liu and Chan 2013; Zhao and Wang 2016, 2019; Hu et al. 2018). From 1979 to 1997, an average of 12.7 TCs occurred in the WNP basin during JJA. This number dropped to 11.0 TCs during 1998–2016—a statistically significant reduction. The WNPMI has decreased from 3.8 during 1979–97 to 3.5 during 1998–2016, although this difference is not significant. This difference is partly manifested by changes in tropical Pacific easterlies and the associated large-scale circulation system (e.g., a weakening WNP monsoon and a westward shift of the TUTT) accompanied by the CP La Niña like pattern and the cool PDO phase as shown in Fig. 4. Together with a significant decrease of WNP TC counts during 1998–2016, we speculate that the relatively weak WNPMI amplitude during 1998–2016 possibly plays a role in contributing to the recent decrease in WNP TC activity. In summary, there appears to be an in-phase climatological relationship between the WNPSM and TCs over the WNP basin, both in terms of a strong association between them during the whole period and a match between interdecadal changes in TC counts and WNPSM amplitude.

We next examine the number of ITCs and OTCs over the WNP basin. On average, during JJA, there were 9.2 ITCs during 1979–97 and 7.5 ITCs during 1998–2016, accounting for about ~72% and ~68% of the total JJA TC frequency during 1979–97 and 1998–2016, respectively (Table 2). The decrease in ITCs from 1979–97 to 1998–2016 is significant. This again indicates the impact of the WNPSM on TC genesis over the WNP basin. In addition, the significant recent reduction in the total number of WNP TCs is dominated by the significant decrease of ITCs during recent decades (Figs. 2 and 5). In contrast, the total number of OTCs between the two subperiods remains virtually unchanged (Fig. 5, Table 2). On average, there are 3.6 OTCs during 1979–97 and 3.5 OTCs during 1998–2016. The decrease in TCs and ITCs is likely due to interdecadal changes in large-scale factors (e.g., low-level relative vorticity, midlevel moisture, and vertical wind shear) in association with changes in the large-scale atmosphere–ocean system (e.g., a weakened monsoon circulation, a westward-shifted TUTT) (Liu and Chan 2013; Wu et al. 2015; Hu et al. 2018; Zhao and Wang 2016, 2019; Zhao et al. 2019) (Fig. 4). However, the physical mechanism for the stability of the OTC counts between the two subperiods merits further investigation.

b. *Recent increase in strength of the interannual relationship between the WNPSM and TCs*

There is an insignificant correlation (0.29) between the WNPMI and TCs during 1979–97, but the correlation is significant (0.68) over the more recent period from 1998–2016 (Fig. 2a, Table 3). This strengthened relationship between the WNPMI and the total TC

TABLE 1. Annual-averaged TC counts for strong and weak western North Pacific summer monsoon (WNPSM) years and the difference between them, respectively, for the periods of 1979–97 and 1998–2016. Double asterisks indicate that the difference is significant at the 95% confidence level.

Subperiod	Extreme WNPSM years	Averaged TC count	Strong minus weak WNPSM years
1979–97	Strong: 1985, 1986, 1990, 1994	13.3	1.8
	Weak: 1983, 1988, 1995, 1996	11.5	
1998–2016	Strong: 2001, 2004, 2012	14.3	6.8**
	Weak: 1998, 2007, 2008, 2010	7.5	

TABLE 2. Annual-averaged total TC counts, ITC counts and OTC counts during 1979–97, 1998–2016, and the whole period from 1979 to 2016. The differences (1998–2016 minus 1979–97) are also listed. Double asterisks indicate that the difference is significant at the 95% confidence level.

	Total TC counts	ITC counts	OTC counts
1979–97	12.7	9.2	3.6
1998–2016	11.0	7.5	3.5
1979–2016	11.9	8.3	3.6
Difference	−1.7**	−1.7**	−0.1

count also manifests itself in an increased relationship between the total TC count and 850-hPa winds over the WNPSM region (Fig. 6). During 1998–2016, the region with significant correlations covers most of the WNPSM, while the area with significant correlations is much smaller during 1979–97. The recent increased interannual relationship between the WNPMI and TC counts over the WNP basin is also demonstrated by a significant difference of TC counts during 1998–2016 and an insignificant difference of TC counts during 1979–97 between strong and weak WNPSM years. During the period of 1979–97, the difference in JJA average TC counts between the strong and weak WNPSM years is an insignificant decrease of 1.8 TCs, while there is a significant decrease of 6.8 TCs between the strong and weak WNPSM years during the period of 1998–2016 (Table 1).

We next investigate changes in the interannual variability of ITCs and OTCs over the WNP basin and how they contribute to interdecadal changes in the interannual relationship between the WNPMI and the total number of WNP TCs. We begin by calculating correlations between the WNPMI and both ITCs and OTCs for the whole period from 1979–2016 as well as the two subperiods from 1979–97 and 1998–2016, respectively. As shown in Fig. 5 and Table 3, there is a significant association between the WNPMI and ITCs during the whole period as well as the two subperiods, indicating that the WNPSM plays a major role in controlling ITCs over the WNP basin. The correlation coefficients are 0.77, 0.80, and 0.76 during 1979–2016, 1979–97, and 1998–2016, respectively. In contrast, the relationship between the WNPMI and OTC counts shows a significant interdecadal change (Fig. 5, Table 3). During 1979–97, OTC frequency significantly negatively correlates at −0.65 with the WNPMI, while the relationship between OTC and WNPMI is insignificant from 1998–2016 ($r = -0.21$). Together with the significant negative correlation of −0.61 between ITC and OTC counts during the period from 1979–97, a hypothesis can be proposed that the WNPSM was possibly a driving mechanism for ITCs and OTCs during 1979–97. Considering a comparable role of

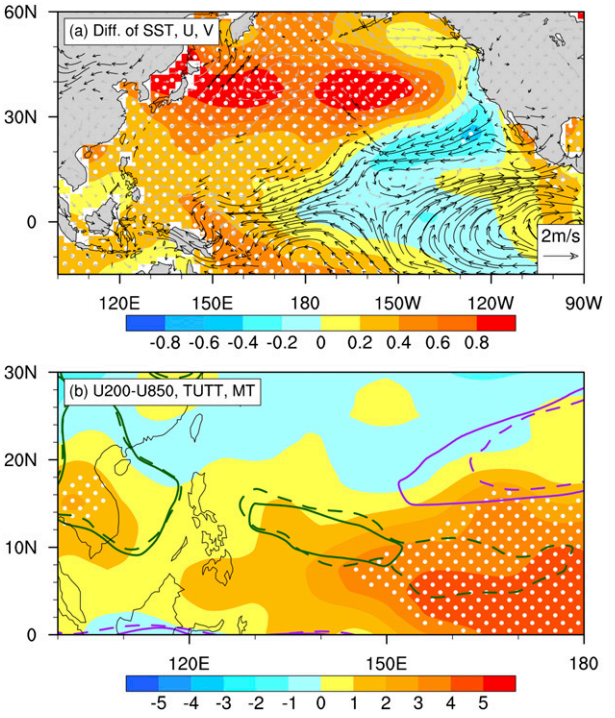

FIG. 4. (a) Summer (JJA) differences (1998–2016 minus 1979–97) in average SST (shading) and 850-hPa wind (vectors). (b) Summer (JJA) differences (1998–2016 minus 1979–97) in zonal vertical wind shear between 200 and 850 hPa (shading; m s^{-1}). The summer (JJA) TUTT (purple lines) and WNPMT (green lines) are identified by relative vorticity of 3×10^{-6} s^{-1} at 200 and 850 hPa, respectively, for 1998–2016 (solid lines) and 1979–97 (dashed lines). White dots and black vectors denote differences significant at a 95% confidence level.

ITCs and OTCs in contributing to the interannual variability of total WNP TCs during 1979–97 (Table 4), a decrease of the in-phase relationship between the total number of WNP TCs and the WNPMI during 1979–97 can be largely explained by the significant positive (negative) correlation between ITCs (OTCs) and the WNPMI (Table 3). In contrast, from 1998 to 2016, there is a strong correlation of 0.78 between ITCs and total WNP TCs and a weak correlation of 0.20 between OTCs and total WNP TCs (Table 4), implying that the interannual variability of the total TC frequency is mainly due to the interannual variability of ITCs during the recent decades. In summary, the recent enhanced interannual relationship between the WNPMI and total TC counts over the WNP basin is largely due to the interdecadal change in the interannual relationship between OTC counts and the WNPMI.

The changes of the interannual relationship between the WNPMI and OTCs are closely linked to changes in the large-scale circulation system controlling OTCs between the two subperiods. In this study, we mainly focus

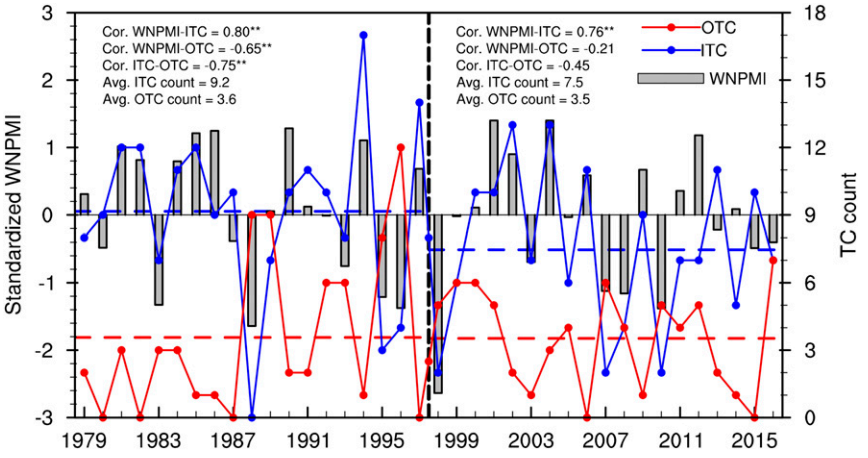

FIG. 5. Time series of standardized summer (JJA) average WNPMI (gray bars), ITC (blue line), and OTC (red line) counts during 1979–2016. The dashed lines indicate the average value during 1979–97 and 1998–2016. The correlation coefficients among WNPMI, ITCs, and OTCs during the two subperiods are also listed. Double asterisks indicate statistical significance at a 95% confidence level.

on two important large-scale circulation systems: the WNPSM and the TUTT. During 1979–97, and as noted earlier, a significant correlation of −0.65 between OTCs and the WNPMI is observed (Figs. 5 and 7a, Table 3), indicating a significant impact of the WNPSM on OTCs over the WNP basin. This was further confirmed by the significant negative correlation between ITCs and OTCs over the WNP basin during 1979–97 (Fig. 5, Table 4). However, during recent decades, the change of OTCs over the WNP basin is found to be primarily associated with changes in the TUTT, with a significant correlation of 0.79 between the OTC and TUTT from 1998 to 2016 (Fig. 7b, Table 3). There is a weakened covariability of the large-scale circulation system affecting ITCs and OTCs during recent decades. This is further reflected by an insignificant correlation between the TUTT and the WNPMI (correlation coefficient is −0.01) from 1998 to 2016 (Fig. 7b). Correspondingly, OTCs have an insignificant correlation of −0.45 with ITCs during 1998–2016 (Fig. 5, Table 4). In summary, the WNPSM plays an important role in controlling ITCs during both subperiods, while there appear to be two different large-scale circulation systems controlling OTCs during the two subperiods. During 1979–97, the WNPSM is the primary driver of OTCs, but the TUTT becomes an important player in modulating OTCs during 1998–2016.

Moreover, we also use the averaged 850-hPa positive relative vorticity over the monsoon region following Molinari and Vollaro (2013) to measure the WNPSM intensity. The WNPSM intensity as calculated following the Molinari and Vollaro (2013) methodology correlates at 0.81 with the WNPMI during 1979–2016. We find almost identical results between the WNPSM intensity and TCs over the WNP basin when using the Molinari and Vollaro (2013) definition. A significant interdecadal change in the interannual relationship between WNPSM intensity and total TC frequency over the WNP basin is also found using the Molinari and Vollaro (2013) definition, with a significant correlation of 0.56 during 1998–2016 and an insignificant correlation of −0.07 during 1979–97. Moreover, a robust and significant association between the WNPSM intensity and ITC counts is observed regardless of the climate regime considered. The

TABLE 3. Correlation coefficients between WNPMI (TUTTI) and TC counts for 1979–97, 1998–2016, and the whole period from 1979 to 2016. Values in boldface are significant at the 95% confidence level.

	WNPMI			TUTTI		
	1979–97	1998–2016	1979–2016	1979–97	1998–2016	1979–2016
ITC counts	**0.80**	**0.76**	**0.77**	0.01	−0.27	−0.21
OTC counts	**−0.65**	−0.21	**−0.46**	0.20	**0.79**	0.35
Total TC counts	0.29	**0.68**	**0.51**	0.27	0.25	0.09

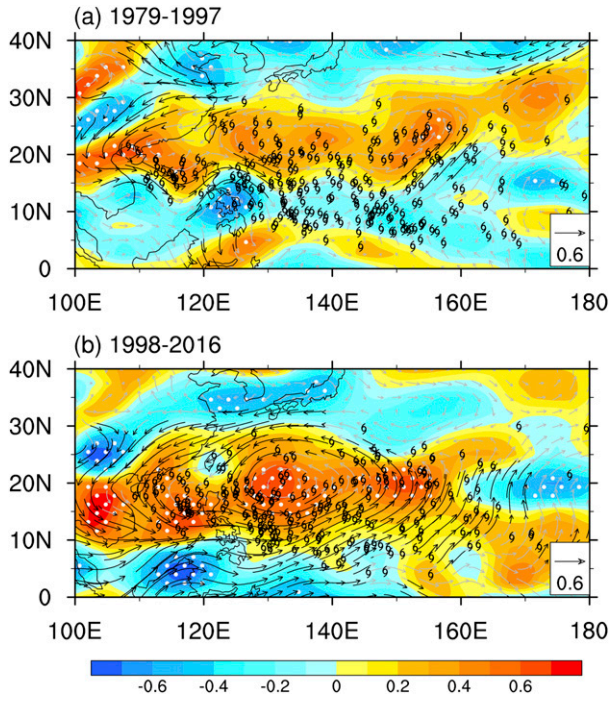

FIG. 6. Correlation patterns of total TC counts and 850-hPa relative vorticity (shading) and wind (vectors) for the periods (a) 1979–97 and (b) 1998–2016. Also plotted are the locations of TC formation. White dots and black vectors represent significant correlations at the 95% confidence level.

correlations are 0.78, 0.70, and 0.74 during 1979–97, 1998–2016, and 1979–2016, respectively. A significant interdecadal change in the interannual relationship between the WNPSM intensity and OTC counts over the WNP basin is also found. There is a significant correlation of −0.89 between WNPSM intensity and OTCs from 1979–97, while the correlation is an insignificant −0.31 from 1998 to 2016. Therefore, consistent results are found using these two definitions for separating ITCs and OTCs over the WNP basin in terms of climatological features of ITCs and OTCs as well as their relationship with large-scale conditions (e.g., WNPSM, TUTT, and ENSO). These findings suggest that the results are not sensitive to the definition of ITCs and OTCs and further raise our confidence of changes in the relationship between the WNPSM and TCs over the WNP basin.

4. Possible explanations for the associated recent enhanced relationship

The interannual variation of the WNPSM is closely linked to ENSO (Wang et al. 2001; Wang and Chan 2002; Camargo and Sobel 2005). We find a significant correlation of 0.33 between the WNPMI and Niño-3.4 during 1979–2016 (Fig. 2b). The WNPMI has a significant correlation of 0.46 with Niño-3.4 during 1998–2016, whereas the correlation is insignificant (0.20) during 1979–97. The correlation between the WNPMI and EMI has also increased from 1979–97 (0.33) to 1998–2016 (0.62), indicating that the recent increased relationship between the WNPSM and ENSO is mainly due to increasing CP ENSO events. A similar result can be found between ENSO and TCs, with an increased EMI–TC association during recent decades (Fig. 2b). Recent studies have suggested that the prevalence of ENSO type is closely related to decadal variations of the mean Pacific Ocean state. These changes over the more recent period (1998–2016) are associated with the PDO phase change from warm to cool, along with more frequent La Niña and CP El Niño events (Verdon and Franks 2006; Kao and Yu 2009; Xiang et al. 2013; Cai et al. 2015). We speculate that the increased association between WNPMI and TCs over the WNP basin is likely closely associated with an increasing occurrence of CP ENSO events and a PDO phase shift from warm to cool (Chan and Zhou 2005; Hu et al. 2018; Zhao and Wang 2016, 2019; Zhao et al. 2016).

During 1979–97, both ITCs and OTCs are closely associated with ENSO, although the total TC frequency over the WNP basin and ENSO has a weak association as shown in Fig. 2b. Figure 8 shows both the ITC–SST and OTC–SST correlation patterns during 1979–97. ITCs (OTCs) have a significant positive (negative) correlation with SST over the tropical central-eastern Pacific, indicating that EP ENSO events significantly impact both ITCs and OTCs. The correlation between 850-hPa winds and ITCs (OTCs) exhibits a significant cyclonic (anticyclonic) circulation pattern primarily covering the WNPSM region. This out-of-phase relationship is further confirmed by a high pattern correlation. A pattern correlation of |0.6| is thought to be a reasonable lower limit for significance (Wilks 2006). The ITC–SST and OTC–SST maps have a pattern

TABLE 4. Correlation coefficients between ITC, OTC, and total TC counts for 1979–97, 1998–2016, and the whole period from 1979 to 2016. Values in boldface are significant at the 95% confidence level.

	ITC counts			OTC counts		
	1979–97	1998–2016	1979–2016	1979–97	1998–2016	1979–2016
OTC counts	**−0.75**	**−0.45**	**−0.61**	—	—	—
Total TC counts	0.44	**0.78**	**0.64**	0.26	0.20	0.22

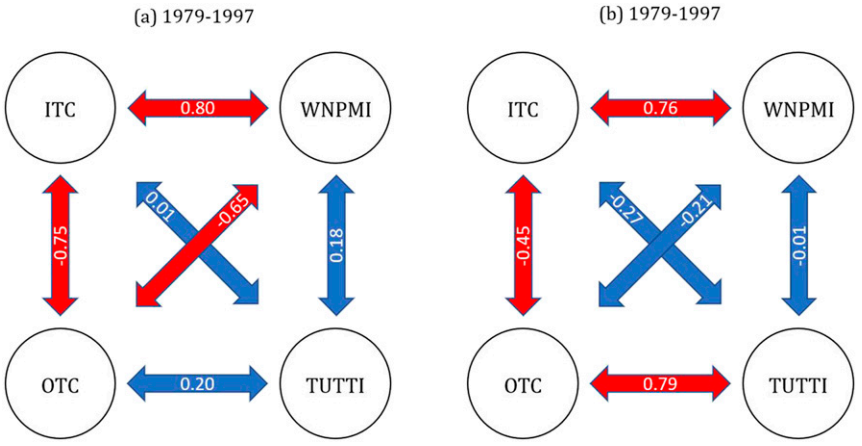

FIG. 7. Correlation coefficients between WNP ITCs, OTCs, and two large-scale circulation systems: the WNPSM (represented by the WNPMI) and the TUTT (represented by the TUTTI) for the periods (a) 1979–97 and (b) 1998–2016. Correlation coefficients in red arrows are significant at the 95% confidence level.

correlation of −0.90. Similarly, pattern correlations of −0.90 (−0.67) between ITC-850 hPa u wind (v wind) and OTC-850 hPa u wind (v wind) are observed. The WNPMI 850-hPa wind correlation pattern shares a very similar positive (negative) correlation pattern as the ITC (OTC) 850-hPa wind during 1979–97 (Fig. 9a). The magnitudes of both pattern correlations are greater than 0.90. Both ITCs and OTCs are closely associated with changes of the WNPSM in response to EP ENSO events. During 1979–97, changes in ITCs and OTCs are closely associated with the conventional EP ENSO-like SST pattern through a change in the WNPSM (Figs. 5 and 8).

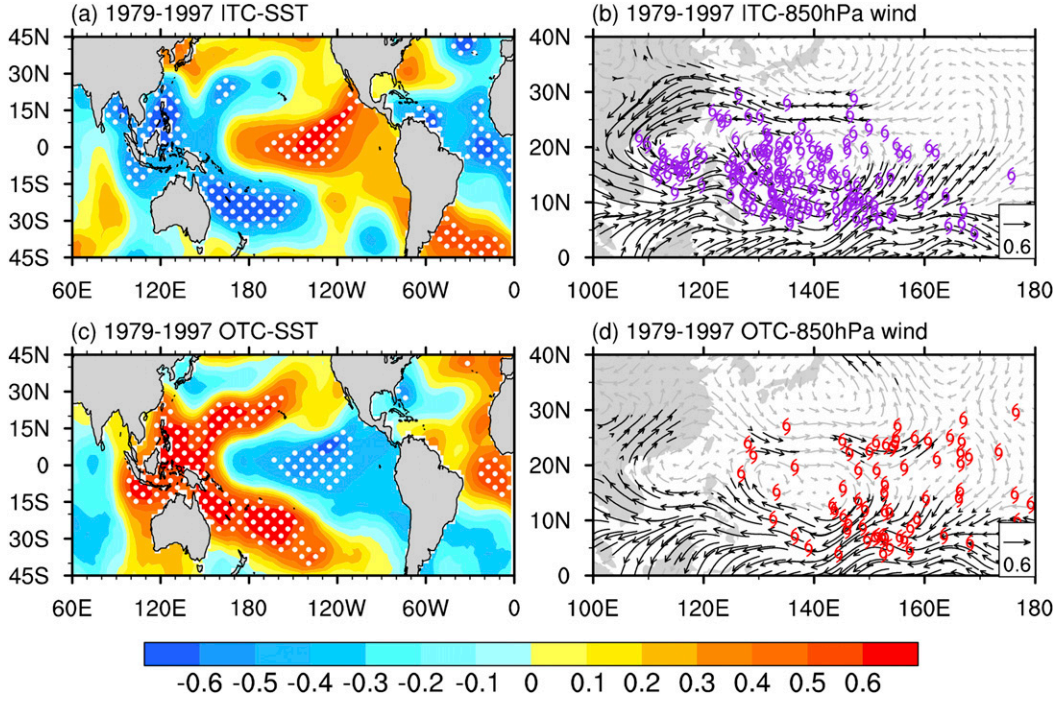

FIG. 8. Correlation patterns (a) between SST and ITC and (c) between SST and OTC during the period of 1979–97. (b),(d) As in (a) and (c), but for correlation patterns (b) between 850-hPa wind and ITCs along with ITC formation locations (purple markers) and (d) between 850-hPa wind and OTCs along with ITC formation locations (red markers). White dots and black vectors denote correlations significant at a 95% confidence level.

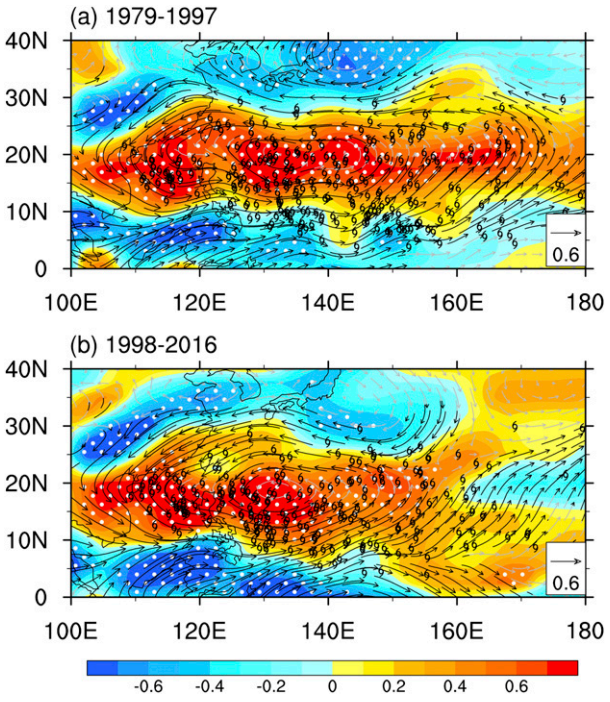

FIG. 9. Correlation patterns of WNPMI and 850-hPa relative vorticity (shading) and wind (vectors) for the periods (a) 1979–97 and (b) 1998–2016. Also displayed are all TC formations. White dots and black vectors represent significant correlations at a 95% confidence level.

During 1998–2016, the ITC–SST and OTC–SST correlations show a CP ENSO-like pattern (Fig. 10) with significant correlations over the tropical CP region. Significant correlations are found between the EMI and ITCs (0.73) and between EMI and OTCs (−0.46) over the WNP basin, implying that CP ENSO events play an important role in controlling ITCs and OTCs during recent decades. However, CP ENSO events show a distinct impact on ITCs and OTCs, which is mainly demonstrated by considerable differences between the ITC-wind and OTC-wind correlation patterns (Fig. 10). Pattern correlations of −0.48 (−0.21) between ITC 850-hPa u wind (v wind) and OTC 850-hPa u wind (v wind) are observed during 1998–2016. Similar results are found between ITC (OTC) 200-hPa wind correlation patterns, with pattern correlations of −0.44 (−0.33) between ITC 200-hPa u wind (v wind) and OTC 200-hPa u wind (v wind), respectively (figure not shown). The change of ITCs during recent decades is mainly controlled by the WNPSM, similar to what occurred from 1979–97. This is further confirmed by high pattern correlations between ITC and u wind at 850 hPa ($r = 0.90$) and between ITC and v wind at 850 hPa ($r = 0.76$) between 1979–97 and 1998–2016 (Figs. 9 and 10). In contrast, the correlations between OTC and 850-hPa wind (200-hPa wind) display significant anticyclonic (cyclonic) circulation patterns over the eastern WNP region (Figs. 10 and 11), which appears to be consistent with a westward shift of the TUTT during recent decades. The TUTT is significantly negatively correlated with the EMI ($r = -0.50$). The TUTTI–SST (TUTTI–200-hPa wind) correlation pattern is very similar to the OTC–SST (OTC–200-hPa wind) correlation pattern as shown in Fig. 10 (Fig. 11), with a corresponding pattern coefficient of 0.94 (0.92). The annual OTC frequency over the WNP basin is further found to be strongly correlated with the TUTTI ($r = 0.79$).

These analyses suggest that the WNPSM remains an important driver of interannual variability of ITCs during recent decades, while OTCs in recent decades are not significantly impacted by the WNPMI but are controlled by changes in the TUTT. However, our results found that these two circulation features both are closely associated with the changes of ENSO conditions during 1998–2016. There are no significant correlations between the WNPMI and TUTTI during either of the two subperiods. This indicates that the impact of CP ENSO events on the WNPSM and TUTTI seem to be independent and deserve more investigation using numerical simulations.

To further understand the relative contributions of large-scale factors associated with the changes in the large-scale circulation affecting OTCs over the WNP basin during both subperiods, we adopted the genesis potential index (GPI) developed by Emanuel and Nolan (2004) with the following expression:

$$\mathrm{GPI} = |10^5\xi|^{3/2}\left(\frac{H}{50}\right)^3\left(\frac{V_{\mathrm{Pot}}}{70}\right)^3(1+0.1V_{\mathrm{Shear}})^{-2}, \quad (2)$$

where ξ is the 850-hPa absolute vorticity (s^{-1}), H is the 600-hPa relative humidity (%), V_{Pot} is the potential intensity (PI) ($m\,s^{-1}$), providing a theoretical upper bound on TC intensity (Bister and Emanuel 2002), and V_{Shear} is the vertical wind shear, computed as the magnitude of the vector difference between 850 and 200 hPa ($m\,s^{-1}$). The total GPI is consistent with the distribution of OTCs during both subperiods but especially for 1979–97 (Fig. 12). During 1979–97 (1998–2016), there is an interannual correlation between the total GPI over the MDR and OTCs of 0.88 (0.50). These correlation coefficients are significant, although the correlation coefficient during 1998–2016 is substantially smaller than that during 1979–97. Nevertheless, the GPI has skill in representing OTC genesis counts during both subperiods, which increases our confidence in investigating the relative contributions of large-scale factors to the changes in OTC counts for both subperiods.

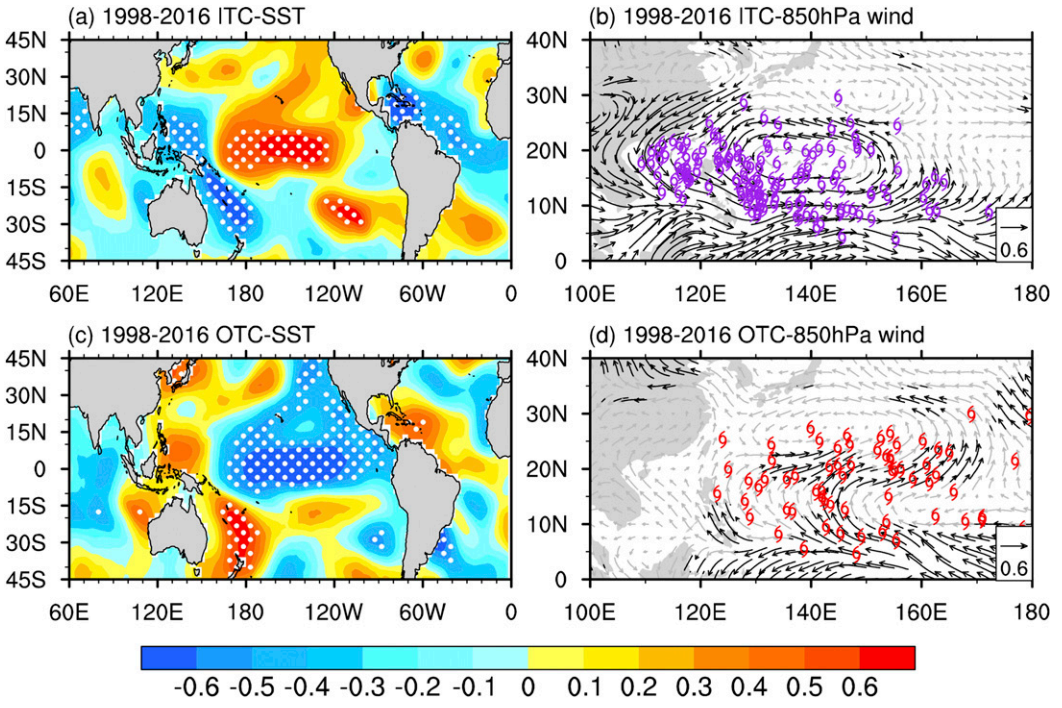

FIG. 10. As in Fig. 8, but for 1998–2016.

The respective roles of each of the four factors included in the GPI in contributing to OTCs are assessed in a similar manner to what has been done in previous studies (Camargo et al. 2009; Jiang et al. 2012; Hu et al. 2018; Zhao et al. 2014, 2015a,b, 2019). The anomalous GPI is calculated by varying one variable but keeping the other three variables at their climatological values. They are referred to as GPI-RHUM, GPI-VOR,

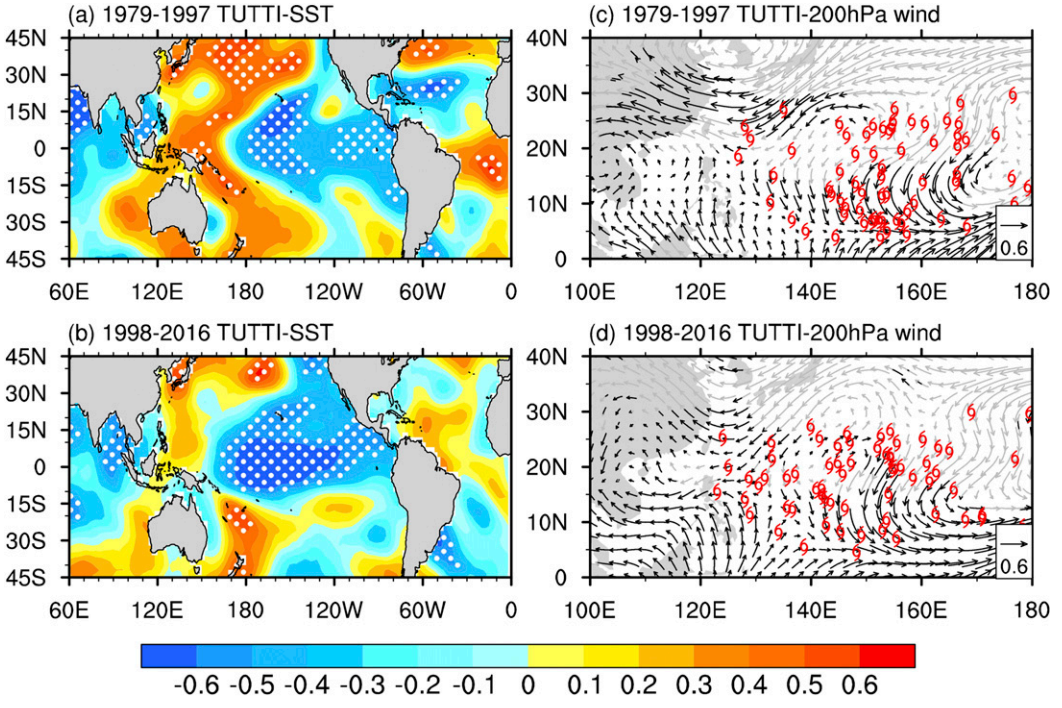

FIG. 11. Correlation patterns between the TUTTI and SST for (a) 1979–97 and (b) 1998–2016. (c),(d) As in (a) and (b), but for 200-hPa wind. Red typhoon symbols in (c) and (d) denote OTC formation locations. White dots and black vectors represent values that are significant at the 95% confidence level.

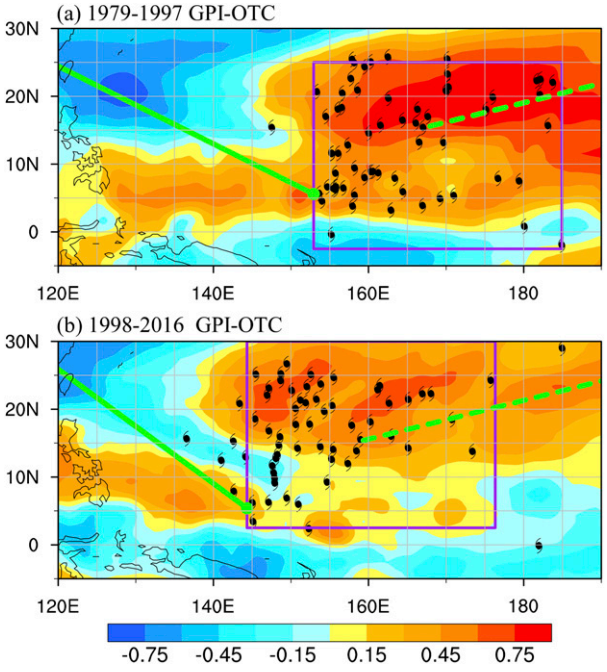

FIG. 12. Correlation pattern of boreal summer (JJA) averaged GPI and OTC counts (shading) during (a) 1979–97 and (b) 1998–2016. The purple boxes are the main development region (MDR) for OTC genesis during 1979–97 (5°S–25°N, 153°E–175°W) and 1998–2016 (2.5°–27.5°N, 144°–176°E). The OTCs are plotted with typhoon markers. The eastern locations of the WNPMT axis, WNPMT, and TUTT axis are plotted by green points, a green solid line, and a green dashed line, respectively.

GPI-VWS, and GPI-PI, respectively, indicating the distinct contributions from the midlevel relative humidity, low-level absolute vorticity, vertical wind shear, and PI. The GPI with all four varying variables is referred to as GPI-Total. Note that the annual GPI-Total, GPI-RHUM, GPI-VOR, GPI-VWS, and GPI-PI are calculated relative to the annual WNPMT as in Fig. 1 and then averaged over the main development region (MDR) for OTCs over the WNP basin covering 5°S–25°N, 153°E–175°W and 2.5°–27.5°N, 144°–176°E during 1979–97 and 1998–2016, respectively.

As shown in Table 5, only GPI-RHUM and GPI-VWS during 1979–97 have a significant positive correlation with OTC counts, with correlation coefficients of 0.51 and 0.60, respectively. Midlevel humidity and vertical wind shear play an important role in controlling OTC genesis during 1979–97. Further examination shows that VWS plays a more important role in modulating OTC counts due to the larger amplitude of GPI-VWS than GPI-RHUM over the MDR (0.8 vs 1.4). Additionally, the WNPMI is found to be significantly correlated with the GPI-VWS but does not correlate significantly with GPI-RHUM. Moreover, both GPI-RHUM and GPI-VWS do not correlate significant with the TUTTI. In summary, vertical wind shear appears to be the most important factors in controlling OTC counts during 1979–97. Changes of vertical wind shear during 1979–97 are found to be mainly due to changes in 850-hPa winds (figure not shown). A plausible cause can be summarized that OTC genesis during 1979–97 is mainly controlled by the WNPMT, through changes in low-level winds that significantly modulate vertical wind shear. In contrast, during 1998–2016, only GPI-RHUM has a significant correlation (r = 0.57) with OTC counts. Meanwhile, the GPI-RHUM significantly correlated with the TUTTI (r = 0.46) but did not correlate significantly with the WNPMI (r = −0.33). In this sense, midlevel relative humidity associated with changes in the TUTT seems to be the most important factor in modulating OTC counts over the WNP basin during 1998–2016. Furthermore, we find that the recent association between midlevel moisture and OTC genesis over the WNP basin is possibly linked to changes in the subtropical high during the latter period. The different underlying physical mechanisms driving OTC genesis during the two subperiods will be studied in future work.

5. Summary and conclusions

This study examines the relationship between the WNPSM and WNP TC frequency during the boreal summer (JJA) from 1979 to 2016. The interannual variability of the WNPSM intensity in this study is measured by the WNPMI defined by Wang and Fan (1999). Consistent with previous studies on the importance of the WNP monsoon circulation on WNP TC frequency

TABLE 5. Correlation coefficients between OTC counts/WNPMI/TUTTI and total GPI (GPI-Total) and GPI with varying low-level vorticity (GPI-VOR), 600-hPa relative humidity (GPI-RHUM), vertical wind shear (GPI-VWS), and potential intensity (GPI-PI) averaged over the MDR during 1979–97 (P1) and 1998–2016 (P2). Values in boldface are significant at the 95% confidence level.

	GPI-Total		GPI-VOR		GPI-RHUM		GPI-VWS		GPI-PI	
	P1	P2	P1	P2	P1	P2	P1	P2	P1	P2
OTC counts	**0.88**	**0.50**	0.42	−0.05	**0.51**	**0.57**	**0.60**	0.42	0.38	0.38
WNPMI	**−0.53**	0.09	−0.38	0.41	−0.31	−0.33	**−0.49**	**−0.56**	−0.09	−0.30
TUTTI	**0.5/**	**0.77**	0.21	0.15	0.45	**0.46**	0.20	**0.51**	0.33	0.37

(Wang et al. 2001; Wang and Chan 2002; Camargo and Sobel 2005; Zhao et al. 2011; Choi et al. 2016), there is a significant correlation between the WNPMI and total WNP TC frequency during 1979–2016 (Fig. 2a). This significant association is found to be mainly due to a recent enhanced interannual relationship between the WNPMI and the total number of WNP TCs during 1998–2016 ($r = 0.68$) compared with during 1979–97 ($r = 0.29$) (Fig. 2a).

Tropical cyclone formation both within and outside of the WNPMT (e.g., ITC or OTC) are considered to further explore the change in the interannual relationship between TCs and the WNPSM. The interdecadal change of the interannual relationship between the WNPSM and OTCs over the WNP basin is closely associated with changes in the large-scale circulation system affecting OTCs over the WNP basin. A robust and significant interannual relationship between ITC counts and the WNPSM between the two subperiods (Figs. 5 and 7) implies the great importance of the WNPSM on changes in the interannual variability of ITCs during both subperiods. In contrast, OTCs show a significant negative correlation ($r = -0.65$) with the WNPSM during 1979–97 but show a weak negative correlation ($r = -0.21$) with the WNPSM during 1998–2016, implying that the WNPSM had a significant impact on OTCs over the WNP basin during 1979–97 but has had little impact on OTCs over the WNP basin during 1998–2016. Changes of OTCs over the WNP basin during 1998–2016 appear to be mainly controlled by the TUTT, since there is a strong association between TUTT intensity and OTC frequency over the WNP basin. Correlation analyses conducted herein suggest that interannual changes of ITCs (OTCs) during 1979–97 (1998–2016) are closely associated with SST over the tropical eastern (central) Pacific (Figs. 2b, 5, 8, and 10). This implies that the interdecadal change in the interannual relationship between the WNPMI and total TC frequency over the WNP is found to be closely associated with both shifting ENSO conditions and the PDO phase transition. During 1979–97 with prevailing EP ENSO events and a PDO warm phase, interannual changes of OTCs over the WNP basin were mainly controlled by changes in the WNPSM but not with the TUTT (Fig. 7). In contrast, the interannual change of OTCs during 1998–2016 was largely dominated by the TUTT (Fig. 7). GPI budget analyses suggest that OTC genesis during 1979–97 is mainly controlled by the WNPMT through changes in low-level winds and thus significant modulation of vertical wind shear, while the midlevel relative humidity associated with changes in the TUTT seem to be the most important factor in modulating OTC counts over the WNP basin during 1998–2016. More observations and numerical simulations are necessary to further elucidate the physical mechanisms driving these observed changes. The results of this study suggest that both changes in the amplitude of the WNPSM and its relationship with TCs/ITCs/OTCs over the WNP basin in response to climate regime shifts are important for an improved understanding of future TC frequency over the WNP basin.

Acknowledgments. We thank the three anonymous reviewers as well as the editor for helpful comments that significantly improved this manuscript. This research was jointly supported by the National Natural Science Foundation of China (Grants 41675072, 41922033, and 41730961), the Natural Science Foundation of Jiangsu Province (Grants BK20181412), the QingLan Project of Jiangsu Province (R2017Q01), the National Basic Research Program of China (2015CB452802), the project of the "Six Talent Peaks Project in Jiangsu Province" (2019-JY-100), and the Priority Academic Program Development of Jiangsu Higher Education Institutions (PAPD). P. Klotzbach would like to acknowledge a grant from the G. Unger Vetlesen Foundation.

REFERENCES

Aiyyer, A. R., and J. Molinari, 2003: Evolution of mixed Rossby–gravity waves in idealized MJO environments. *J. Atmos. Sci.*, **60**, 2837–2855, https://doi.org/10.1175/1520-0469(2003)060<2837:EOMRWI>2.0.CO;2.

Ashok, K., S. K. Behera, S. A. Rao, H. Weng, and T. Yamagata, 2007: El Niño Modoki and its possible teleconnection. *J. Geophys. Res.*, **112**, C11007, https://doi.org/10.1029/2006JC003798.

Bister, M., and K. A. Emanuel, 2002: Low frequency variability of tropical cyclone potential intensity. 1. Interannual to interdecadal variability. *J. Geophys. Res.*, **107**, 4801, https://doi.org/10.1029/2001JD000776.

Briegel, L. M., and W. M. Frank, 1997: Large-scale influences on tropical cyclogenesis in the western North Pacific. *Mon. Wea. Rev.*, **125**, 1397–1413, https://doi.org/10.1175/1520-0493(1997)125<1397:LSIOTC>2.0.CO;2.

Cai, W., and Coauthors, 2015: ENSO and greenhouse warming. *Nat. Climate Change*, **5**, 849–859, https://doi.org/10.1038/nclimate2743.

Camargo, S. J., and A. H. Sobel, 2005: Western North Pacific tropical cyclone intensity and ENSO. *J. Climate*, **18**, 2996–3006, https://doi.org/10.1175/JCLI3457.1.

——, K. A. Emanuel, and A. H. Sobel, 2007a: Use of a genesis potential index to diagnose ENSO effects on tropical cyclone genesis. *J. Climate*, **20**, 4819–4834, https://doi.org/10.1175/JCLI4282.1.

——, A. H. Sobel, A. G. Barnston, and K. A. Emanuel, 2007b: Tropical cyclone genesis potential index in climate models. *Tellus*, **59A**, 428–443, https://doi.org/10.1111/j.1600-0870.2007.00238.x.

——, M. C. Wheeler, and A. H. Sobel, 2009: Diagnosis of the MJO modulation of tropical cyclogenesis using an empirical

index. *J. Atmos. Sci.*, **66**, 3061–3074, https://doi.org/10.1175/2009JAS3101.1.

Cao, X., S. Chen, G. Chen, and R. Wu, 2016: Intensified impact of northern tropical Atlantic SST on tropical cyclogenesis frequency over the western North Pacific after the late 1980s. *Adv. Atmos. Sci.*, **33**, 919–930, https://doi.org/10.1007/s00376-016-5206-z.

Chan, J. C. L., 2005: Interannual and interdecadal variations of tropical cyclone activity over the western North Pacific. *Meteor. Atmos. Phys.*, **89**, 143–152, https://doi.org/10.1007/S00703-005-0126-Y.

——, and W. Zhou, 2005: PDO, ENSO and the early summer monsoon rainfall over south China. *Geophys. Res. Lett.*, **32**, L08810, https://doi.org/10.1029/2004GL022015.

Chan, S. C., and J. L. Evans, 2002: Comparison of the structure of the ITCZ in the west Pacific during the boreal summers of 1989–93 using AMIP simulations and ECMWF reanalysis. *J. Climate*, **15**, 3549–3568, https://doi.org/10.1175/1520-0442(2002)015<3549:COTSOT>2.0.CO;2.

Chen, G., and R. Huang, 2009: Interannual variations in mixed Rossby–gravity waves and their impacts on tropical cyclogenesis over the western North Pacific. *J. Climate*, **22**, 535–549, https://doi.org/10.1175/2008JCLI2221.1.

——, and C.-Y. Tam, 2010: Different impacts of two kinds of Pacific Ocean warming on tropical cyclone frequency over the western North Pacific. *Geophys. Res. Lett.*, **37**, L01803, https://doi.org/10.1029/2009GL041708.

Chen, T.-C., S.-P. Weng, N. Yamazaki, and S. Kiehne, 1998: Interannual variation in the tropical cyclone formation over the western North Pacific. *Mon. Wea. Rev.*, **126**, 1080–1090, https://doi.org/10.1175/1520-0493(1998)126<1080:IVITTC>2.0.CO;2.

——, S. Wang, and M. Yen, 2006: Interannual variation of the tropical cyclone activity over the western North Pacific. *J. Climate*, **19**, 5709–5720, https://doi.org/10.1175/JCLI3934.1.

Choi, J. W., B. J. Kim, R. Zhang, K. J. Park, J. Y. Kim, Y. Cha, and J. C. Nam, 2016: Possible relation of the western North Pacific monsoon to the tropical cyclone activity over western North Pacific. *Int. J. Climatol.*, **36**, 3334–3345, https://doi.org/10.1002/joc.4558.

Chou, C., J.-Y. Tu, and J.-Y. Yu, 2003: Interannual variability of the western North Pacific summer monsoon: Differences between ENSO and non-ENSO years. *J. Climate*, **16**, 2275–2287, https://doi.org/10.1175/2761.1.

Chu, J.-H., C. R. Sampson, A. S. Levine, and E. Fukada, 2002: The Joint Typhoon Warning Center tropical cyclone best tracks 1945–2000. Joint Typhoon Warning Center Rep., https://www.metoc.navy.mil/jtwc/products/best-tracks/tc-bt-report.html.

Dickinson, M., and J. Molinari, 2002: Mixed Rossby–gravity waves and western Pacific tropical cyclogenesis. Part I: Synoptic evolution. *J. Atmos. Sci.*, **59**, 2183–2196, https://doi.org/10.1175/1520-0469(2002)059<2183:MRGWAW>2.0.CO;2.

Emanuel, K., 2018: 100 years of progress in tropical cyclone research. *A Century of Progress in Atmospheric and Related Sciences: Celebrating the American Meteorological Society Centennial*, *Meteor. Monogr.*, No. 59, 15.1–15.68, https://doi.org/10.1175/AMSMONOGRAPHS-D-18-0016.1.

——, and D. S. Nolan, 2004: Tropical cyclone activity and the global climate system. *26th Conf. on Hurricanes and Tropical Meteorology*, Miami, FL, Amer. Meteor. Soc., 240–241, https://ams.confex.com/ams/26HURR/techprogram/paper_75463.htm.

Frank, W. M., 1987: Tropical cyclone formation. *A Global View of Tropical Cyclones*, R. L. Elsberry, Ed., University of Chicago Press, 53–90.

——, and P. E. Roundy, 2006: The role of tropical waves in tropical cyclogenesis. *Mon. Wea. Rev.*, **134**, 2397–2417, https://doi.org/10.1175/MWR3204.1.

Goldenberg, S. B., and L. J. Shapiro, 1996: Physical mechanisms for the association of El Niño and West African rainfall with Atlantic major hurricane activity. *J. Climate*, **9**, 1169–1187, https://doi.org/10.1175/1520-0442(1996)009<1169:PMFTAO>2.0.CO;2.

Gray, W. M., 1968: Global view of the origin of tropical disturbances and storms. *Mon. Wea. Rev.*, **96**, 669–700, https://doi.org/10.1175/1520-0493(1968)096<0669:GVOTOO>2.0.CO;2.

——, 1975: Tropical cyclone genesis. Department of Atmospheric Science Paper 234, Colorado State University, 121 pp.

——, 1979: Hurricanes: Their formation, structure and likely role in the tropical circulation. D. B. Shaw, Ed., *Meteorology over the Tropical Oceans*, Royal Meteorological Society, 155–218.

——, 1984: Atlantic seasonal hurricane frequency. Part I: El Niño and 30 mb quasi-biennial oscillation influences. *Mon. Wea. Rev.*, **112**, 1649–1668, https://doi.org/10.1175/1520-0493(1984)112<1649:ASHFPI>2.0.CO;2.

——, 1998: The formation of tropical cyclones. *Meteor. Atmos. Phys.*, **67**, 37–69, https://doi.org/10.1007/BF01277501.

Han, R., and Coauthors, 2016: An assessment of multimodel simulations for the variability of western North Pacific tropical cyclones and its association with ENSO. *J. Climate*, **29**, 6401–6423, https://doi.org/10.1175/JCLI-D-15-0720.1.

Harr, P. A., and J. C. L. Chan, 2005: Monsoon impacts on tropical cyclone variability. *The Global Monsoon System: Research and Forecast*, C. P. Chang, B. Wang, and N. C. Lau, Eds., WMO, 512–542.

He, H., J. Yang, L. Wu, D. Gong, B. Wang, and M. Gao, 2017: Unusual growth in intense typhoon occurrences over the Philippine Sea in September after the mid-2000s. *Climate Dyn.*, **48**, 1893–1910, https://doi.org/10.1007/s00382-016-3181-9.

Holland, G. J., 1995: Scale interaction in the western Pacific monsoon. *Meteor. Atmos. Phys.*, **56**, 57–79, https://doi.org/10.1007/BF01022521.

Hong, C.-C., Y.-H. Li, T. Li, and M.-Y. Lee, 2011: Impacts of central Pacific and eastern Pacific El Niños on tropical cyclone tracks over the western North Pacific. *Geophys. Res. Lett.*, **38**, L16712, https://doi.org/10.1029/2011GL048821.

——, Y.-K. Wu, and T. Li, 2016: Influence of climate regime shift on the interdecadal change in tropical cyclone activity over the Pacific Basin during the middle to late 1990s. *Climate Dyn.*, **47**, 2587–2600, https://doi.org/10.1007/s00382-016-2986-x.

Hsu, P.-C., P.-S. Chu, H. Murakami, and X. Zhao, 2014: An abrupt decrease in the late-season typhoon activity over the western North Pacific. *J. Climate*, **27**, 4296–4312, https://doi.org/10.1175/JCLI-D-13-00417.1.

Hu, C., C. Zhang, S. Yang, D. Chen, and S. He, 2018: Perspective on the northwestward shift of autumn tropical cyclogenesis locations over the western North Pacific from shifting ENSO. *Climate Dyn.*, **51**, 2455–2465, https://doi.org/10.1007/S00382-017-4022-1.

Huang, B., and Coauthors, 2015: Extended reconstructed sea surface temperature version 4 (ERSST.v4). Part I: Upgrades and intercomparisons. *J. Climate*, **28**, 911–930, https://doi.org/10.1175/JCLI-D-14-00006.1.

Huangfu, J., R. Huang, W. Chen, T. Feng, and L. Wu, 2017: Interdecadal variation of tropical cyclone genesis and its relationship to the monsoon trough over the western North Pacific. *Int. J. Climatol.*, **37**, 3587–3596, https://doi.org/10.1002/joc.4939.

Jiang, X., and Coauthors, 2012: Simulation of the intraseasonal variability over the eastern Pacific ITCZ in climate models. *Climate Dyn.*, **39**, 617–636, https://doi.org/10.1007/s00382-011-1098-x.

——, B. Xiang, M. Zhao, T. Li, S.-J. Lin, Z. Wang, and J.-H. Chen, 2018: Intraseasonal tropical cyclone genesis prediction in a global coupled model system. *J. Climate*, **31**, 6209–6227, https://doi.org/10.1175/JCLI-D-17-0454.1.

Kanamitsu, M., W. Ebisuzaki, J. Woollen, S. Yang, J. J. Hnilo, M. Fiorino, and G. L. Potter, 2002: NCEP–DOE AMIP-II reanalysis (R-2). *Bull. Amer. Meteor. Soc.*, **83**, 1631–1643, https://doi.org/10.1175/BAMS-83-11-1631.

Kao, H. Y., and J. Y. Yu, 2009: Contrasting eastern-Pacific and central-Pacific types of ENSO. *J. Climate*, **22**, 615–632, https://doi.org/10.1175/2008JCLI2309.1.

Kim, H. M., P. J. Webster, and J. A. Curry, 2009: Impact of shifting patterns of Pacific Ocean warming on North Atlantic tropical cyclones. *Science*, **325**, 77–80, https://doi.org/10.1126/science.1174062.

Knutson, T. R., and Coauthors, 2010: Tropical cyclones and climate change. *Nat. Geosci.*, **3**, 157–163, https://doi.org/10.1038/ngeo779.

Lander, M. A., 1994: An exploratory analysis of the relationship between tropical storm formation in the western North Pacific and ENSO. *Mon. Wea. Rev.*, **122**, 636–651, https://doi.org/10.1175/1520-0493(1994)122<0636:AEAOTR>2.0.CO;2.

Li, T., B. Wang, B. Wu, T. Zhou, C. P. Chang, and R. Zhang, 2017: Theories on formation of an anomalous anticyclone in western North Pacific during El Niño: A review. *J. Meteor. Res.*, **31**, 987–1006, https://doi.org/10.1007/s13351-017-7147-6.

Liu, K. S., and J. C. L. Chan, 2013: Inactive period of western North Pacific tropical cyclone activity in 1998–2011. *J. Climate*, **26**, 2614–2630, https://doi.org/10.1175/JCLI-D-12-00053.1.

Liu, W., and Coauthors, 2015: Extended reconstructed sea surface temperature version 4 (ERSST. v4): Part II. Parametric and structural uncertainty estimations. *J. Climate*, **28**, 931–951, https://doi.org/10.1175/JCLI-D-14-00007.1.

Lyon, B., and S. J. Camargo, 2009: The seasonally-varying influence of ENSO on rainfall and tropical cyclone activity in the Philippines. *Climate Dyn.*, **32**, 125–141, https://doi.org/10.1007/s00382-008-0380-z.

Maue, R. N., 2011: Recent historically low global tropical cyclone activity. *Geophys. Res. Lett.*, **38**, L14803, https://doi.org/10.1029/2011GL047711.

McBride, J. L., 1995: Tropical cyclone formation. *Global Perspectives on Tropical Cyclones*, R. L. Elsberry, Ed., World Meteorological Organization, 63–105.

——, and R. Zehr, 1981: Observational analysis of tropical cyclone formation. Part II: Comparison of non-developing versus developing systems. *J. Atmos. Sci.*, **38**, 1132–1151, https://doi.org/10.1175/1520-0469(1981)038<1132:OAOTCF>2.0.CO;2.

Molinari, J., and D. Vollaro, 2013: What percentage of western North Pacific tropical cyclones form within the monsoon trough? *Mon. Wea. Rev.*, **141**, 499–505, https://doi.org/10.1175/MWR-D-12-00165.1.

Murakami, H., and B. Wang, 2010: Future change of North Atlantic tropical cyclone tracks: Projection by a 20-km-mesh global atmospheric model. *J. Climate*, **23**, 2699–2721, https://doi.org/10.1175/2010JCLI3338.1.

Nolan, D. S., Y. Moon, and D. P. Stern, 2007: Tropical cyclone intensification from asymmetric convection: Energetics and efficiency. *J. Atmos. Sci.*, **64**, 3377–3405, https://doi.org/10.1175/JAS3988.1.

Reed, R. J., and E. E. Recker, 1971: Structure and properties of synoptic-scale wave disturbances in the equatorial western Pacific. *J. Atmos. Sci.*, **28**, 1117–1133, https://doi.org/10.1175/1520-0469(1971)028<1117:SAPOSS>2.0.CO;2.

Ritchie, E. A., 1995: Mesoscale aspects of tropical cyclone formation. Ph.D. dissertation, Monash University, 167 pp.

——, and G. J. Holland, 1999: Large-scale patterns associated with tropical cyclogenesis in the western Pacific. *Mon. Wea. Rev.*, **127**, 2027–2043, https://doi.org/10.1175/1520-0493(1999)127<2027:LSPAWT>2.0.CO;2.

Shapiro, L. J., 1977: Tropical storm formation from easterly waves: A criterion for development. *J. Atmos. Sci.*, **34**, 1007–1022, https://doi.org/10.1175/1520-0469(1977)034<1007:TSFFEW>2.0.CO;2.

——, 1987: Month-to-month variability of the Atlantic tropical circulation and its relationship to tropical storm formation. *Mon. Wea. Rev.*, **115**, 2598–2614, https://doi.org/10.1175/1520-0493(1987)115<2598:MTMVOT>2.0.CO;2.

Sobel, A. H., and E. D. Maloney, 2000: Effect of ENSO and the MJO on western North Pacific tropical cyclones. *Geophys. Res. Lett.*, **27**, 1739–1742, https://doi.org/10.1029/1999GL011043.

Tippett, M. K., S. J. Camargo, and A. H. Sobel, 2011: A Poisson regression index for tropical cyclone genesis and the role of large-scale vorticity in genesis. *J. Climate*, **24**, 2335–2357, https://doi.org/10.1175/2010JCLI3811.1.

Tomita, T., T. Yoshikane, and T. Yasunari, 2004: Biennial and lower-frequency variability observed in the early summer climate in the western North Pacific. *J. Climate*, **17**, 4254–4266, https://doi.org/10.1175/JCLI3200.1.

Vecchi, G. A., and B. J. Soden, 2007: Effect of remote sea surface temperature change on tropical cyclone potential intensity. *Nature*, **450**, 1066–1077, https://doi.org/10.1038/nature06423.

Verdon, D. C., and S. W. Franks, 2006: Long-term behaviour of ENSO: Interactions with the PDO over the past 400 years inferred from paleoclimate records. *Geophys. Res. Lett.*, **33**, L06712, https://doi.org/10.1029/2005GL025052.

Wallace, J. M., 1971: Spectral studies of tropospheric wave disturbances in the tropical western Pacific. *Rev. Geophys.*, **9**, 557–612, https://doi.org/10.1029/RG009i003p00557.

Walsh, K. J. E., and Coauthors, 2015: Hurricanes and climate: The U.S. CLIVAR working group on hurricanes. *Bull. Amer. Meteor. Soc.*, **96**, 997–1017, https://doi.org/10.1175/BAMS-D-13-00242.1.

Wang, B., and Z. Fan, 1999: Choice of South Asian summer monsoon indices. *Bull. Amer. Meteor. Soc.*, **80**, 629–638, https://doi.org/10.1175/1520-0477(1999)080<0629:COSASM>2.0.CO;2.

——, and J. C. L. Chan, 2002: How strong ENSO events affect tropical storm activity over the western North Pacific. *J. Climate*, **15**, 1643–1658, https://doi.org/10.1175/1520-0442(2002)015<1643:HSEEAT>2.0.CO;2.

——, and X. Zhou, 2008: Climate variation and prediction of rapid intensification in tropical cyclones in the western North Pacific. *Meteor. Atmos. Phys.*, **99**, 1–16, https://doi.org/10.1007/s00703-006-0238-z.

——, R. Wu, and R. Lukas, 1999: Roles of the western North Pacific wind variation in thermocline adjustment and ENSO phase transition. *J. Meteor. Soc. Japan*, **77**, 1–16, https://doi.org/10.2151/jmsj1965.77.1_1.

——, ——, and X. Fu, 2000: Pacific–East Asian teleconnection: How does ENSO affect East Asian climate? *J. Climate*, **13**, 1517–1536, https://doi.org/10.1175/1520-0442(2000)013<1517:PEATHD>2.0.CO;2.

——, ——, and K. M. Lau, 2001: Interannual variability of the Asian summer monsoon: Contrasts between the Indian and the western North Pacific–East Asian monsoons. *J. Climate*, **14**, 4073–4090, https://doi.org/10.1175/1520-0442(2001)014<4073:IVOTAS>2.0.CO;2.

Wang, C., and L. Wu, 2016: Interannual shift of the tropical upper-tropospheric trough and its influence on tropical cyclone for-

mation over the western North Pacific. *J. Climate*, **29**, 4203–4211, https://doi.org/10.1175/JCLI-D-15-0653.1.

——, and ——, 2018: Projection of North Pacific tropical upper-tropospheric trough in CMIP5 models: Implications for changes in tropical cyclone formation locations. *J. Climate*, **31**, 761–774, https://doi.org/10.1175/JCLI-D-17-0292.1.

——, B. Wang, and L. Wu, 2019: Abrupt breakdown of the predictability of early season typhoon frequency at the beginning of the twenty-first century. *Climate Dyn.*, **52**, 3809–3822, https://doi.org/10.1007/s00382-018-4350-9.

Wang, H., and Coauthors, 2014: How well do global climate models simulate the variability of Atlantic tropical cyclones associated with ENSO? *J. Climate*, **27**, 5673–5692, https://doi.org/10.1175/JCLI-D-13-00625.1.

Wang, X., and H. Liu, 2016: PDO modulation of ENSO effect on tropical cyclone rapid intensification in the western North Pacific. *Climate Dyn.*, **46**, 15–28, https://doi.org/10.1007/s00382-015-2563-8.

Wilks, D. S., 2006: *Statistical Methods in the Atmospheric Sciences*. 2nd ed. Academic Press, 648 pp.

Wu, L., Z. P. Wen, R. H. Huang, and R. G. Wu, 2012: Possible linkage between the monsoon trough variability and the tropical cyclone activity over the western North Pacific. *Mon. Wea. Rev.*, **140**, 140–150, https://doi.org/10.1175/MWR-D-11-00078.1.

——, C. Wang, and B. Wang, 2015: Westward shift of western North Pacific tropical cyclogenesis. *Geophys. Res. Lett.*, **42**, 1537–1542, https://doi.org/10.1002/2015GL063450.

Wu, R., and B. Wang, 2000: Interannual variability of summer monsoon onset over the western North Pacific and the underlying processes. *J. Climate*, **13**, 2483–2501, https://doi.org/10.1175/1520-0442(2000)013<2483:IVOSMO>2.0.CO;2.

Xiang, B., B. Wang, and T. Li, 2013: A new paradigm for the predominance of standing Central Pacific warming after the late 1990s. *Climate Dyn.*, **41**, 327–340, https://doi.org/10.1007/s00382-012-1427-8.

——, and Coauthors, 2015: Beyond weather time-scale prediction for Hurricane Sandy and Super Typhoon Haiyan in a global climate model. *Mon. Wea. Rev.*, **143**, 524–535, https://doi.org/10.1175/MWR-D-14-00227.1.

Yokoi, S., and Y. N. Takayabu, 2009: Multi-model projection of global warming impact on tropical cyclone genesis frequency over the western North Pacific. *J. Meteor. Soc. Japan*, **87**, 525–538, https://doi.org/10.2151/jmsj.87.525.

——, ——, and J. C. Chan, 2009: Tropical cyclone genesis frequency over the western North Pacific simulated in medium-resolution coupled general circulation models. *Climate Dyn.*, **33**, 665–683, https://doi.org/10.1007/s00382-009-0593-9.

Yu, J. Y., M. M. Lu, and S. T. Kim, 2012: A change in the relationship between tropical central Pacific SST variability and the extratropical atmosphere around 1990. *Environ. Res. Lett.*, **7**, 034025, https://doi.org/10.1088/1748-9326/7/3/034025.

Zehnder, J. A., 1991: The interaction of planetary-scale tropical easterly waves with topography: A mechanism for the initiation of tropical cyclones. *J. Atmos. Sci.*, **48**, 1217–1230, https://doi.org/10.1175/1520-0469(1991)048<1217:TIOPST>2.0.CO;2.

Zehr, R. M., 1992: Tropical cyclogenesis in the western North Pacific. NOAA Tech. Rep. NESDIS 61, U.S. Department of Commerce, 181 pp.

Zhang, Q., L. Wu, and Q. Liu, 2009: Tropical cyclone damages in China 1983–2006. *Bull. Amer. Meteor. Soc.*, **90**, 489–495, https://doi.org/10.1175/2008BAMS2631.1.

Zhao, H., and G. B. Raga, 2014: The influence of large-scale circulations on the extremely inactive tropical cyclone activity in 2010 over the western North Pacific. *Atmósfera*, **27**, 353–365, https://doi.org/10.1016/S0187-6236(14)70034-7.

——, and ——, 2015: On the distinct interannual variability of tropical cyclone activity over the eastern North Pacific. *Atmósfera*, **28**, 161–178, https://doi.org/10.20937/ATM.2015.28.03.02.

——, and C. Wang, 2016: Interdecadal modulation on the relationship between ENSO and typhoon activity during the late season in the western North Pacific. *Climate Dyn.*, **47**, 315–328, https://doi.org/10.1007/s00382-015-2837-1.

——, and ——, 2019: On the relationship between ENSO and tropical cyclones in the western North Pacific during the boreal summer. *Climate Dyn.*, **52**, 275–288, https://doi.org/10.1007/S00382-018-4136-0.

——, L. Wu, and W. Zhou, 2011: Interannual changes of tropical cyclone intensity in the western North Pacific. *J. Meteor. Soc. Japan*, **89**, 243–253, https://doi.org/10.2151/jmsj.2011-305.

——, P.-S. Chu, P.-C. Hsu, and H. Murakami, 2014: Exploratory analysis of extremely low tropical cyclone activity during the late-season of 2010 and 1998 over the western North Pacific and the South China Sea. *J. Adv. Model. Earth Syst.*, **6**, 1141–1153, https://doi.org/10.1002/2014MS000381.

——, X. Jiang, and L. Wu, 2015a: Modulation of northwest Pacific tropical cyclone genesis by the intraseasonal variability. *J. Meteor. Soc. Japan*, **93**, 81–97, https://doi.org/10.2151/jmsj.2015-006.

——, R. Yoshida, and G. B. Raga, 2015b: Impact of the Madden–Julian oscillation on western North Pacific tropical cyclogenesis associated with large-scale patterns. *J. Appl. Meteor. Climatol.*, **54**, 1413–1429, https://doi.org/10.1175/JAMC-D-14-0254.1.

——, X. Jiang, and L. Wu, 2016: Boreal summer synoptic-scale waves over the western North Pacific in multi-model simulations. *J. Climate*, **29**, 4487–4508, https://doi.org/10.1175/JCLI-D-15-0696.1.

——, S. Chen, P. J. Klotzbach, and G. B. Raga, 2018a: Impact of the extended boreal summer intraseasonal oscillation on western North Pacific tropical cloud cluster genesis productivity. *J. Climate*, **31**, 9175–9191, https://doi.org/10.1175/JCLI-D-18-0113.1.

——, X. Duan, G. B. Raga, and P. J. Klotzbach, 2018b: Changes in characteristics of rapidly intensifying western North Pacific tropical cyclones related to climate regime shifts. *J. Climate*, **31**, 8163–8179, https://doi.org/10.1175/JCLI-D-18-0029.1.

——, S. Chen, G. B. Raga, P. J. Klotzbach, and L. Wu, 2019: Recent decrease in genesis productivity of tropical cloud clusters over the western North Pacific. *Climate Dyn.*, **52**, 5819–5831, https://doi.org/10.1007/S00382-018-4477-8.

Zhou, B., and X. Cui, 2014: Interdecadal change of the linkage between the North Atlantic Oscillation and the tropical cyclone frequency over the western North Pacific. *Sci. China Earth Sci.*, **57**, 2148–2155, https://doi.org/10.1007/s11430-014-4862-z.

Zhou, X., and B. Wang, 2007: Transition from an eastern Pacific upper-level mixed Rossby–gravity wave to a western Pacific tropical cyclone. *Geophys. Res. Lett.*, **34**, L24801, https://doi.org/10.1029/2007GL031831.

Zong, H., and L. Wu, 2015a: Re-examination of tropical cyclone formation in monsoon troughs over the western North Pacific. *Adv. Atmos. Sci.*, **32**, 924–934, https://doi.org/10.1007/s00376-014-4115-2.

——, and ——, 2015b: Synoptic-scale influences on tropical cyclone formation within the western North Pacific monsoon trough. *Mon. Wea. Rev.*, **143**, 3421–3433, https://doi.org/10.1175/MWR-D-14-00321.1.